Engineering Microbiology 4 (2024) 100166

Contents lists available at ScienceDirect

Engineering Microbiology

journal homepage: www.elsevier.com/locate/engmic

Original Research Article

Functional analysis of the whole CYPome and Fdxome of *Streptomyces venezuelae* ATCC 15439

Shuai Li[a], Zhong Li[a], Guoqiang Zhang[a], Vlada B. Urlacher[b], Li Ma[a,*], Shengying Li[a,c,*]

[a] State Key Laboratory of Microbial Technology, Shandong University, Qingdao, Shandong 266237, China
[b] Institute of Biochemistry, Heinrich-Heine-University Düsseldorf, Universitätsstraße 1, Düsseldorf 40225, Germany
[c] Laboratory for Marine Biology and Biotechnology, Qingdao Marine Science and Technology Center, Qingdao, Shandong 266237, China

ARTICLE INFO

Keyword:
Streptomyces
Cytochrome P450 enzymes
CYPome
Ferredoxin
Fdxome
PikC

ABSTRACT

Cytochrome P450 enzymes (CYPs or P450s) and ferredoxins (Fdxs) are ubiquitously distributed in all domains of life. Bacterial P450s are capable of catalyzing various oxidative reactions with two electrons usually donated by Fdxs. Particularly in *Streptomyces*, there are abundant P450s that have exhibited outstanding biosynthetic capacity of bioactive metabolites and great potential for xenobiotic metabolisms. However, no systematic study has been conducted on physiological functions of the whole cytochrome P450 complement (CYPome) and ferredoxin complement (Fdxome) of any *Streptomyces* strain to date, leaving a significant knowledge gap in microbial functional genomics. Herein, we functionally analyze the whole CYPome and Fdxome of *Streptomyces venezuelae* ATCC 15439 by investigating groups of single and sequential P450 deletion mutants, single P450 overexpression mutants, and Fdx gene deletion or repression mutants. Construction of an unprecedented P450-null mutant strain indicates that none of P450 genes are essential for *S. venezuelae* in maintaining its survival and normal morphology. The non-housekeeping Fdx1 and housekeeping Fdx3 not only jointly support the cellular activity of the prototypic P450 enzyme PikC, but also play significant regulatory functions. These findings significantly advance the understandings of the native functionality of P450s and Fdxs as well as their cellular interactions.

1. Introduction

Streptomyces are Gram-positive filamentous bacteria and constitute the largest genus of actinobacteria [1]. These microorganisms are among the richest sources of natural products with diverse biological and pharmaceutical activities, including many applied antibiotics, antifungals, antitumor agents, immunosuppressants, herbicides, and insecticides [2]. In particular, >60 % of antibiotics in clinical use, such as streptomycin, erythromycin, tetracycline and vancomycin, are originated from *Streptomyces* [3,4].

Cytochrome P450 enzymes (CYPs or P450s) are heme-containing monooxygenases that are widely distributed in all kingdoms of life [5]. This superfamily of catalytically versatile metalloenzymes are extensively involved in xenobiotics metabolism and natural product biosynthesis [6–8]. Due to differences in ecological niche and adapted evolution, microbial P450s exhibit great functional diversity. In mycobacterial species, P450s facilitate the utilization of host lipids or synthesis of new lipids to adapt to the living environment, whereas in fungi P450s play a crucial role in the biosynthesis of ergosterol [9,10]. As the genius natural product producers, *Streptomyces* spp. are particularly P450-rich microorganisms partially because the P450-introduced functional groups (*e.g.*, hydroxyl and epoxide groups) not only increase the structural diversity of natural products, but also enhance the water solubility, biological activity, and bioavailability of the resulting products [8]. For example, *Streptomyces coelicolor* A3(2), *Streptomyces avermitilis* MA-4680, and *Streptomyces venezuelae* ATCC 15439 have 18 [11] (with three P450 genes located within a biosynthetic gene cluster, BGC), 33 [12] (four), and 25 [13] (three) P450 genes on their genomes, respectively. Each cytochrome P450 complement (CYPome or P450ome) accounts for approximately 0.2~0.4 % of the corresponding whole genome sequence.

Despite the diversity and abundance of *Streptomyces* P450 enzymes, only 184 species (with a majority of them being natural product biosynthetic P450s) have been functionally identified until 2017, only accounting for about 2.4 % of the total number of *Streptomyces* CYPs [6]. Although many *Streptomyces*-derived P450s have been investigated for their activities to modify exogenous compounds for practical application purposes [14–17], the physiological functions of a majority of *Streptomyces* P450s remain largely unknown. A fundamental question has yet to be answered is whether there exists any housekeeping P450 gene in *Streptomyces*. To the best of our knowledge, there has no systematic functional analysis of a whole *Streptomyces* CYPome so far, leading to the lack

* Corresponding authors at: State Key Laboratory of Microbial Technology, Shandong University, Qingdao, Shandong 266237, China.
E-mail addresses: maliqd@sdu.edu.cn (L. Ma), lishengying@sdu.edu.cn (S. Li).

https://doi.org/10.1016/j.engmic.2024.100166
Received 25 June 2024; Received in revised form 7 August 2024; Accepted 13 August 2024
Available online 13 August 2024

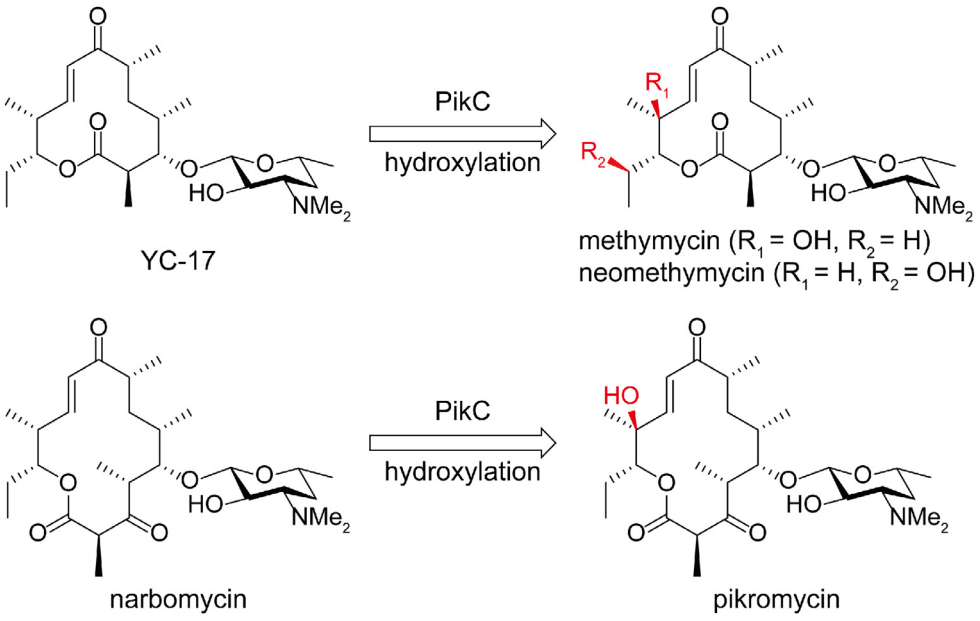

Fig. 1. The physiological reactions catalyzed by PikC. PikC hydroxylates the C-10 and C-12 positions of YC-17 almost equally to produce methymycin and neomethymycin, respectively, as well as the C-12 position of narbomycin predominantly to generate pikromycin.

of comprehensive understanding of the native functions of *Streptomyces* P450ome.

The three-component class I P450 system is prevalent in *Streptomyces*, in which an FAD-containing ferredoxin reductase (FdR), a small iron–sulfur protein ferredoxin (Fdx), and a P450 enzyme form a typical electron transfer pathway: NAD(P)H→FdR→Fdx→P450. With the discovery of the first Fdx from *Clostridium pasteurianum* in 1960s [18], the function of Fdx in utilizing Fe–S cluster to shuttle electrons from FdR to P450 has been well studied [19–21]. Moreover, Fdxs are involved in various cellular processes that are essential for cell growth and development. For instance, Fdx can respond to photooxidative stress by regulating the expression of photosynthesis related genes in cyanobacterium *Synechocystis* sp. PCC 6803 [22]. *Escherichia coli* employs Fdx to assemble Fe–S clusters [23]. In *Pseudomonas aeruginosa*, Fdx was reported to be an essential housekeeping gene [24].

According to our genomic analysis, *S. coelicolor* A3(2), *S. avermitilis* MA-4680, and *S. venezuelae* ATCC 15439 have 6 [25], 9 [12], and 7 [13] *fdx* genes, respectively. Our previous studies have determined the optimal electron transport pathways for PikC from *S. venezuelae* ATCC 15439 *in vitro* and revealed some empirical rules for redox partner selectivity of bacterial P450s [26,27]. Notably, the prototypic P450 enzyme PikC is responsible for catalyzing the C-10 and C-12 hydroxylation (almost equally) of the 12-membered ring macrolide YC-17 to produce methymycin and neomethymycin, respectively, as well as the C-12 hydroxylation of the 14-membered ring macrolide narbomycin to generate pikromycin [28] (Fig. 1). However, it remains unclear how PikC interacts with Fdxs inside cells and whether the above-mentioned rules would be different *in vivo* due to multiplicity/complexity of P450s and Fdxs as well as dynamic cellular environments.

To address these important questions, herein, we systematically investigated the *in vivo* functions of the whole CYPome (25 P450 genes) and Fdxome (7 *fdx* genes) of *S. venezuelae* ATCC 15439 by bioinformatics analysis of the complete genomes, transcriptome-guided CRISPR/Cas9 gene knockout [29] and CRISPR/dCas9-based gene interference (CRISPRi) [30] (Fig. S1). Genotyping and phenotyping of 25 single P450 knockout mutants, 21 multi-P450 sequential deletion mutants, a P450-free mutant, and 25 single P450 overexpression mutants, and of 4 single *fdx* knockout mutants, 5 multi-*fdx* sequential deletion mutants, and 3 *fdx* knockdown mutants showed that no P450 gene is essential for the survival of *S. venezuelae* ATCC 15439, and Fdx1 and Fdx3 are responsible for supporting the cellular activity of PikC. The regulatory functions of these two Fdx-encoding genes were also revealed.

2. Materials and methods

2.1. Materials

The chemicals and antibiotics used in this study were purchased from Solarbio (Beijing, China), Sinopharm Chemical Reagent (Beijing, China), and Sangon (Shanghai, China) unless otherwise specified. All restriction enzymes were purchased from Thermo Scientific (Waltham, USA) and Takara (Dalian, China). The ClonExpress Ultra One Step Cloning Kit was obtained from Vazyme (Nanjing, China). PrimeSTAR Max DNA Polymerase (Dalian, China) was used to amplify DNA fragments by PCR reactions. The TRIzol reagent for RNA extraction was bought from Ambion (Waltham, USA). The recombinant DNase I (RNase-free) used to degrade genomic DNA was obtained from Takara (Dalian, China). The PrimeScript™ RT reagent for cDNA preparation and TB Green®Premix Ex Taq™II (Tli RNaseH Plus) for qRT-PCR were purchased from Takara (Dalian, China). Primers were synthesized by Sangon (Qingdao, China). DNA sequencing was performed by TsingKe (Qingdao, China). The BGCs were analyzed by antiSMASH bacterial version [31]. DNAman 7.0 was used for DNA sequence alignment. Protein sequences were aligned by ClustalW and the results were output by ESPript 3.0 [32].

2.2. Strains and culture conditions

All strains used in this study are listed in Table S1. *E. coli* strains were cultured at 37 °C on LB (10 g tryptone, 5 g yeast extract, and 10 g NaCl per liter) agar or in LB liquid media. *S. venezuelae* ATCC 15439 and their derivatives were grown at 30 °C on mannitol soya flour (MS) agar (20 g soy flour, 20 g mannitol, 20 g agar per liter) for sporulation and conjugation. *E. coli* ET12567/pUZ8002 was employed for intergeneric conjugation with *S. venezuelae* in MS medium supplemented with 50 mM $CaCl_2$ and $MgCl_2$ [33]. 2 × YT liquid medium (16 g tryptone, 10 g yeast extract, and 5 g NaCl per liter) was used to culture *S. venezuelae* liquid seed and for genomic DNA (gDNA) preparation. The fermentation media SCM (15 g soluble starch, 20 g soytone, 0.1 g $CaCl_2$, 1.5 g yeast extract, and 10.5 g MOPS per liter, pH 7.2) and ISP4 (10 g soluble starch, 1 g K_2HPO_4, 1 g $MgSO_4{\cdot}7H_2O$, 1 g NaCl, 2 g $(NH_4)_2SO_4$, 2 g $CaCO_3$, and 1 mL trace salts solution per liter, pH 7.2) were used for production of secondary metabolites in *S. venezuelae* strains. For identification of *S. venezuelae* morphological characteristics, MYM agar containing 4 g/L maltose, 4 g/L yeast extract, 10 g/L malt extract and 20 g/L agar was used. MYM liquid medium was used to analyze the

biomass of *Streptomyces*. Antibiotics including apramycin (50 mg mL^{-1}), kanamycin (50 mg mL^{-1}), chloramphenicol (25 mg mL^{-1}), hygromycin (100 mg mL^{-1}), and nalidixic acid (20 mg mL^{-1}) were added when necessary.

2.3. Construction of gene deletion plasmids

All primers used for plasmid construction and clone screening are listed in Table S2. The CRISPR/Cas9 editing template plasmid pKCcas9dO was kindly provided by Prof. Yinhua Lu at Shanghai Normal University. All gene knockout plasmids were derived from the modifications of the CRISPR/Cas9 genome editing plasmid pKCcas9dO [29]. Taking PikC-knockout plasmid construction as an example, the *pikC* gene-specific sgRNA cassette was amplified from pKCcas9dO using primers PikCgRNA-F and PikCgRNA-R. The upstream and downstream homologous arms flanking *pikC* were amplified separately from *S. venezuelae* genomic DNA using primer pairs PikCLA-F/PikCLA-R and PikCRA-F/PikCRA-R. The three amplicons were then joined into the *Spe*I/*Hin*dIII-linearized pKCcas9dO vector using the ClonExpress Ultra One Step Cloning Kit to obtain pKCcas9dOPikC. The correct plasmid was confirmed by PCR and DNA sequencing. All other P450 and *fdx* gene deletion plasmids in this study were constructed similarly by changing the gene-specific sgRNA cassettes and two homologous fragments.

2.4. Construction of gene overexpression plasmids

For gene overexpression in *S. venezuelae*, the target genes were amplified from the genome of *S. venezuelae* using specific primer pairs shown in Table S2 (The CYP183AR1 and CYP183AS1 overexpression plasmids were constructed in our previous study [34]). Next, the target fragments were homologously recombined and inserted into the linear integrative vector pDR4-*kasO*p* (provided by Prof. Weishan Wang at Institute of Microbiology, Chinese Academy of Sciences) digested by *Spe*I/*Kpn*I using ClonExpress Ultra One Step Cloning Kit, resulting in the overexpression plasmids under the strong promoter *kasO*p*. All the constructed plasmids were confirmed by PCR and DNA sequencing using primer pairs M13F-47/M13R-48.

2.5. Construction of gene repression plasmids

CRISPRi plasmids containing sgRNA targeting the specific *fdx* genes were assembled based on the plasmid pSET-dCas9-actII4-NT-S1 [30]. To generate repression plasmids for *fdx2, fdx3*, and *fdx5* (*i.e.*, pSET-dCas9-fdx2, pSET-dCas9-fdx3, and pSET-dCas9-fdx5), the *fdx* gene specific sgRNA cassettes were amplified from pSET-dCas9-actII4-NT-S1 using the forward primers gRNA-dx2 (containing 20 bp specific target sequence of *fdx2*), gRNA-dx3 (containing 20 bp specific target sequence of *fdx3*), gRNA-dx5 (containing 20 bp specific target sequence of *fdx5*), and the reverse primer HA-dCas9-gRNA-R, respectively. Subsequently, each individual PCR product was separately ligated to the *Spe*I/*Eco*RI linearized pSET-dCas9-actII4-NT-S1 vector using ClonExpress Ultra One Step Cloning Kit. The constructed plasmids were confirmed by PCR and DNA sequencing using primer pairs dCas9-YZ-F/dCas9-YZ-R.

2.6. Construction and genotypic confirmation of S. venezuelae mutants

The primers for PCR confirmation of *S. venezuelae* mutants are listed in Table S2. For constructing gene deletion mutant strains, the CRISPR/Cas9 plasmid was transformed from *E. coli* ET12567/pUZ8002 to *S. venezuelae* strain via interspecies conjugation according to standard *Streptomyces* protocols [33]. Then, the conjugants were treated with nalidixic acid and apramycin on MS plates after incubation for 14–16 h at 30 °C and incubated for another 3–5 d at 30 °C. Exoconjugants were then picked up for genomic DNA preparation and confirmation by PCR and DNA sequencing. Finally, correct *S. venezuelae* gene deletion mutants lost the knockout plasmids after multiple rounds of cultivation at 37 °C.

For constructing gene overexpression or gene repression mutant strains, the pDR4-*kasO*p* integrative vector carrying target gene or CRISPRi plasmid were transformed from *E. coli* ET12567/pUZ8002 to *S. venezuelae* via interspecies conjugation. Next, the target conjugants were treated with nalidixic acid and hygromycin (for screening gene overexpression mutants) or apramycin (for screening gene repression mutants) on MS plates after incubation for 14–16 h at 30 °C and incubated for another 3–5 d at 30 °C. The colonies were picked up for confirmation via PCR, DNA sequencing, or qRT-PCR experiments.

2.7. Whole genome sequencing and assembly

Sv-WT and *Sv*-Del23 strain were cultured on MS agar plates at 30 °C for 3 d. Colonies were then transferred to 2 × YT liquid seed media and inoculated in 30 mL volume using 250 mL flasks at 30 °C and 220 rpm. After 24 h cultivation, 30 mL cell pellets were centrifuged for 10 min at 6,000 × *g* at 4 °C, washed three times with an equal volume of sterile water in 50 mL conical tubes, flash-frozen with liquid nitrogen, and delivered with dry ice to BGI Genomics Co., Ltd for DNA extraction, whole genome sequencing, and assembly.

2.8. Biomass measurement

For biomass measurement of the wild-type and mutant *S. venezuelae* strains, a single colony of each strain was inoculated into 30 mL 2 × YT liquid medium. After 24 h, the seed culture was transferred into fresh 30 mL MYM liquid medium in 250 mL flasks at a 100-fold dilution ratio and cultured at 220 rpm, 30 °C. After 3-d cultivation, 10 mL of each sample was harvested in a pre-dried and pre-weighed 50 mL tube by centrifugation at 8,000 × *g* for 5 min. The supernatant was removed and the cell pellet was dried at 75 °C for 24 h to a constant weight. The dry weight of each sample was then measured by calculating the weight difference before and after sample addition.

2.9. Morphological observation and scanning electron microscopy analysis

A single colony of wild-type or P450-inactivated mutants of *S. venezuelae* was cultured in 2 × YT seed medium at 30 °C and 220 rpm for 24 h. The OD_{600} of the seed liquid was then measured using a microplate reader and the initial OD_{600} was normalized to 50. Next, the normalized seed culture was inoculated onto an MYM agar plate for morphological observation and the phenotypes were photographed every 24 h for three consecutive days.

To compare the morphological differentiation of mycelia, field emission scanning electron microscopy (FESEM) was used to take cell images. The collected aerial mycelia or liquid cultured cells (washed once with PBS buffer) grown for 72 h were fixed with 2.5 % glutaraldehyde for 1 h, and then washed twice with PBS buffer. Next, a series of concentrations of ethanol were used to dehydrate the sample, with each dehydration lasting for 15 min. After the sample was fully dried, it was coated with platinum, and the images were taken with FESEM.

2.10. Transcriptional analysis by qRT-PCR

A single colony of *Sv*-WT, *Sv*-Δ*fdx2*-down, *Sv*-Δ*fdx3*-down, and *Sv*-Δ*fdx5*-down was individually picked from MS agar plates and inoculated into 30 mL 2 × YT media and cultured at 30 °C, 220 rpm. The 3 mL of one-day culture was inoculated into 30 mL SCM medium and shaking-incubated for additional 24 and 36 h in triplicate. The RNA samples of *Sv*-Δ*fdx2*-down, *Sv*-Δ*fdx3*-down, and *Sv*-Δ*fdx5*-down mutants were extracted using Trizol (Ambion, USA) and digested with

DNase I (Takara, Dalian, China) to remove genomic DNA contamination. The quality and quantity of RNAs were analyzed using UV spectroscopy and agarose gel electrophoresis. Then, purified RNA samples were reverse-transcribed using PrimeScript™ RT reagent Kit (Takara, Dalian, China). The primers were designed by Primer3Plus online service (Primer3Plus - Pick Primers) and listed in Table S2. Quantitative real-time RT-PCR (qRT-PCR) was carried out using TB Green® Premix Ex Tag™ II (Takara, Dalian, China) in a CFX96 thermal cycler (Bio-Rad, USA). The two-step qRT-PCR reaction program was as follows: 95 ˚C for 30 s, followed by 40 cycles of 95 ˚C for 5 s, and 60 ˚C for 30 s. qRT-PCR analyses were carried out in triplicate. The relative transcription levels of target genes were normalized to *hrdB* (an internal control) and then calculated using the $2^{-\Delta\Delta CT}$ method [35].

2.11. Transcriptome analysis

A single colony of *Sv*-WT and *Sv*-Δ*fdx1* deletion mutant was individually inoculated into 30 mL 2 × YT media, which were shaken at 30 ˚C and 220 rpm. After one-day culture, the seed culture was used to inoculate into 30 mL SCM media in triplicate at a ratio of 1:10. After a 24-h cultivation at 30 ˚C and 220 rpm, the cells from each individual flask were harvested by centrifugation at 6,000 × *g* for 10 min at 4 ˚C in RNase-free tubes. Finally, the cells were flash-frozen with liquid nitrogen and delivered with dry ice to Novogene for mRNA isolation and transcriptome sequencing and analysis. Gene transcript levels at various stages were evaluated using fragments per kilobase (kb) of exon model per million mapped reads (FPKM). Based on a large amount of gene expression data, we defined the expressed genes (FPKM > 1) and silent genes (FPKM < 1). Analysis of differential expression was performed using R package DEseq2 to compare different genes, and a heat map was generated using GraphPad Prism 9.5 with the $\log_2$FoldChange. For expression analysis of P450 genes, transcriptomic sequencing data were collected from the previous work [34]. These data present the expression levels of 25 P450 genes during the transition (24 h) and stationary (48 h) phases of *S. venezuelae* development.

2.12. Analysis of metabolites

A single colony of the wild-type and mutant *S. venezuelae* strains was individually grown on an MS plate and inoculated into 30 mL 2 × YT media and shaking-incubated at 220 rpm and 30 ˚C for one day. After that, 3 mL seed culture was transferred to 30 mL SCM medium or ISP4 medium and cultured at 30 ˚C and 220 rpm for another seven days. For the exogenous YC-17 feeding experiments of the *fdx* mutants, *Sv*-Δ*fdx*1 and *Sv*-Δ*fdx3*-down were fed with 200 μM (final concentration) of YC-17 in 30 mL SCM medium at the time of inoculation at 30 ˚C, 220 rpm for 7-d biotransformation.

For analysis of metabolite profiles of *S. venezuelae* strains, the culture broth of each strain was extracted twice with an equal volume of ethyl acetate. The extract was evaporated *in vacuo*, and re-dissolved in 1 mL of methanol. Then, the extract was analyzed using a reversed phase YMC Triart C-18 column (4.6 mm × 250 mm, 5 μm) on a Thermo UltiMate 3000 instrument with a mobile phase of acetonitrile and deionized water containing 0.1 % trifluoroacetic acid at the flow rate of 1 ml/min. The gradient elution program of acetonitrile in water was as follows: 10 %, 0–1 min; 10–100 %, 1–26 min; 100 %, 26–30 min; 100 %–10 %, 30–31 min; 10 %, 31–33 min. The ultraviolet wavelength was set at 230 nm.

2.13. Statistical analysis

The statistical significance of all inter group differences in this study was tested using two-tailed unpaired Student's *t*-test. $^{*}P < 0.05$, $^{**}P < 0.01$, $^{***}P < 0.001$. *P* value < 0.05 was considered to be statistically significant. GraphPad Prism 9.5 was used to perform statistical analyses.

3. Results

3.1. The CYPome and fdxome of S. venezuelae ATCC 15439

S. venezuelae ATCC 15439 is not only a versatile producer of natural products (especially bioactive macrolides), but also a model strain for studying morphological and physiological differentiation [36]. Despite the reported complete genome sequence of this strain [13], we re-sequenced the whole genome by combining BGISEQ data (904 M, 100 × coverage) and PacBio data (11,788 M, 1,306 × coverage) in order to provide a better blueprint for our studies on CYPome and Fdxome. As a result, the complete genome (9,022,698 bp, GenBank accession number: CP140569) contains 8,422 genes with a GC content of 72.16 %, which is slightly different from the previous genome sequencing results [13] (Table S3). This genome harbors 25 P450 genes, 7 Fdx genes, and 7 FdR genes (Table S4). In *S. venezuelae* ATCC 15439, the P450 genes account for ~0.3 % of the whole genome sequence, which is relatively higher than the corresponding percentage of 0.2 % in *S. coelicolor* A3(2) [11].

The 25 P450s are classified into 14 P450 families (with amino acid sequence homology of > 40 %, Table S4) by Prof. David Nelson [5]. The CYP107 family is the largest P450 family in *S. venezuelae* ATCC 15439 with 6 family members including CYP107L1 (the prototypic bacterial P450 enzyme PikC), CYP107U11, CYP107P10, CYP107L47, CYP107CM1 and CYP107AE11. Other P450 families with more than one family member include CYP183 (CYP183AR1, CYP183AS1 and CYP183B3), CYP154 (CYP154D18, CYP154A41 and CYP154C15), CYP105 (CYP105AC40 and CYP105AC41), and CYP1047 (CYP1047A6 and CYP1047B2). The linear chromosome also harbors nine P450 genes with each from distinct P450 families, encoding CYP245A10, CYP184A13, CYP121A2, CYP125A21, CYP159A7P, CYP163B14, CYP180A24, CYP1251A1 and CYP157A27. Of note, the coding genes of CYP183AR1 and CYP183AS1 neighbor and overlap with each other, as are those of CYP154C15 and CYP157A27.

Next, we sought to map these CYP genes onto the antiSMASH-predicted secondary metabolite BGCs of *S. venezuelae*. As a result, 11 out of 25 P450 genes were found to be located in 8 BGCs (Table S5). Among these P450s, CYP107L1 (*i.e.*, PikC) is well-known for its hydroxylation activities in the pikromycin/(neo)methymycin biosynthetic pathway (Fig. 1) [28,37,38]. In our previous study on biosynthesis of venezuelaenes, CYP183AS1 (*i.e.*, VenC) was characterized to catalyze the four-electron oxidation of venezuelaene A into venezuelaene B, while CYP183AR1 (*i.e.*, VenB) is inactive in this biosynthetic system [34,39]. More recently, we characterized a type I polyketide BGC *ved* responsible for biosynthesis of venediols. However, CYP154A41 encoded by a P450 gene neighboring *ved* (10.8 kb upstream) did not show any activity towards venediols, thus becoming an orphan CYP [40]. For the rest seven putative biosynthetic P450 genes, their function elucidation requires further studies.

With regard to the Fdxome of *S. venezuelae* ATCC 15439, seven Fdx proteins with three different types of Fe–S clusters were identified (Fig. S2, Tables S4 and S6). Based on the conserved amino acids in the Fe–S cluster binding motif(s) [26], we classified Fdx1, Fdx2, Fdx4 and Fdx7 as [3Fe–4S] type Fdxs since all four Fdxs contain the signature motif of $C(X)_5C(X)_nCP$. Putatively, the *fdx5* and *fdx6* genes encode two [7Fe–8S] type Fdxs with two Fe–S cluster binding motifs including $C(X)_nC$ and $C(X)_nC(X)_2C(X)_3CP$, suggesting that these two Fdxs might have mixed [3Fe–4S] and [4Fe–4S] clusters. Fdx3 was predicted as a Rieske protein that contains a single [2Fe–2S] cluster with two histidine nitrogen ligands ($CXHX_{16}CX_2H$) [41].

3.2. Construction of a library of S. venezuelae mutant strains with each single P450 gene deleted

To investigate whether there is any housekeeping P450 gene in *S. venezuelae* ATCC 15439, we individually knocked out each of 25 P450

genes using CRISPR/Cas9-based gene editing technology (Table S1). The knockout vectors were constructed using the pKCcas9dO plasmid as a backbone [29]. The in-frame deletions were confirmed by PCR amplification and DNA sequencing of the 25 mutation regions (Fig. S3). Evidently, none of the single P450 gene deletions affected the viability of each mutant strain, indicating that no P450 gene is required for survival of *S. venezuelae* ATCC 15439 under the tested conditions.

3.3. Construction of a S. venezuelae strain devoid of all P450 genes

Since there is no housekeeping P450 gene in *S. venezuelae* ATCC 15439, we sought to construct a P450-minimal or even P450-free mutant strain by knocking out the 25 P450 genes stepwise. The transcriptome analysis (Fig. S4, Table S7) of the wild-type *S. venezuelae* ATCC 15439 when cultured in SCM medium [34] indicated that most CYP genes were moderately expressed with a FPKM value > 1. However, the transcription levels of *CYP183AS1, CYP105AC40, CYP245A10, CYP1047B2* and *CYP157A27* genes decreased significantly at the stationary growth stage (48 h) to be silent (FPKM value < 1). Of note, the CYP transcriptional levels were one of the key factors to determine the order of sequential P450 gene deletions (*see below*).

To construct a strain with minimal P450ome, we performed multiple rounds of P450 gene knockout and monitored the cumulative effects due to the decreasing number of P450 genes. The order of P450 gene deletions was determined according to the following principles: 1) the CYP families containing any P450 gene(s) involved in natural product biosynthesis were knocked out firstly and successively; and 2) for the rest P450 genes, the ones with higher transcription levels were deleted preferentially. Despite availability of multi-gene knockout tools, we reasoned that a one-by-one gene deletion approach was more suitable for tracking the changes of growth and differentiation as well as secondary metabolism resulted from the removal of each P450 gene. The only two exceptions were the two pairs of overlapping P450 genes, namely, *CYP183AR1* and *CYP183AS1*, and *CYP157A27* and *CYP154C15*, both of which were deleted simultaneously under the guidance of one gRNA. Notably, CYP107L1 (*i.e.*, PikC) is the earliest and most studied P450 enzyme in *S. venezuelae*. Thus, the CYP107 family was selected as the first P450 family to be knocked out. Specifically, *Sv*-Del1 lacking the *CYP107L47* gene was used as the starting point for further P450 gene deletions. Multiple deletion cycles were applied in order to achieve the minimal P450ome. As a result, 21 multi-P450 sequential deletion strains (*Sv*-Del2∼22) and a P450-free strain *Sv*-Del23 were obtained (Fig. 2a, Table S1). These strains again indicate that there is no housekeeping P450 gene in *S. venezuelae* ATCC 15439 (*see below* for more details).

To confirm the genotype of the unprecedented P450-null *Streptomyces* strain, the complete genome of *Sv*-Del23 was sequenced and assembled (GenBank accession number: CP140665). As expected, the 25 P450 genes were confirmed to be completely deleted by comparing the P450 loci of *Sv*-WT and *Sv*-Del23 based on PCR amplification results (Fig. S5). Unexpectedly, according to genome sequence alignment (Fig. 2b), *Sv*-Del23 chromosome lost approximately 0.6 Mbp (AQF52_0010–AQF52_0579, ∼6.7 % of the whole genome) of the left genomic region. A large segment of genes (AQF52_5965–AQF52_8092) underwent inversion and translocation. The region of AQF52_5965–AQF52_5978 had an additional copy. In addition, the terminal inverted repeats (TIRs, AQF52_0001–AQF52_0008 and AQF52_8093–AQF52_8101) at both ends of the *Sv*-WT genome were missing in *Sv*-Del23. To determine the timing of these genomic changes, we analyzed the key regions by PCR amplifications and DNA sequencing for *Sv*-Del1∼23 (Figs. S6 and S7). Surprisingly, the same large-scale chromosomal rearrangements as *Sv*-Del23 were detected in the first CYP107L47 gene deletion mutant *Sv*-Del1. We reasoned that the introduction of CRISPR/Cas9 system might have caused chromosome instability, thus triggering the unwanted off-target effects [42] during deletion of the first P450 gene. It is worth noting that these undesired genomic modifications would unlikely influence our data interpretation and conclusions in this study.

3.4. P450s have no significant impacts on morphological differentiation of S. venezuelae

Previous studies have shown that in many cases the production of secondary metabolites is closely related to the regulatory network of physiological and morphological differentiation in *Streptomyces* [43,44]. For example, the *CYP107U1* gene of *S. coelicolor* plays key roles in aerial hyphae sporulation and heat shock response [45]. To understand the potential functions of *S. venezuelae* P450s on mycelial growth and morphological differentiation, we grew all the single P450-deficient mutants on an MYM agar plate. The spore-bearing hyphae colors and mycelial states of each strain at three different time points (24, 48 and 72 h) were recorded and compared. During the dynamic culture process, the spores of *Sv*-WT germinated and slowly grew upward from the substrate mycelia on MYM agar, breaking through the solid medium to form aerial hyphae. With further development, the aerial hyphae gradually changed from white to gray and the spores were formed at this stage. Compared with the growth phenotype of *Sv*-WT, all single P450 gene knockout mutants grew normally, without apparent bald colony morphology and abnormal spore differentiation (Fig. 2c). Furthermore, we cultured all P450 sequential deletion mutants on MYM agar. Similar to the results of the single knockout mutants, the cumulative deletion of P450 genes also did not cause significant differences in colony phenotype (Fig. 2d). Although the mycelial growth rates and spore accumulation of individual mutants varied, the differences appeared to be random in repeated experiments. Since none of the P450 gene deletions significantly influenced the development of aerial hyphae and sporulation, we conclude that the 25 P450 genes unlikely participate in the regulation of the growth and development of *S. venezuelae* ATCC 15439.

3.5. Growth characteristics and metabolic profiles of the P450-deficient strains

To evaluate the effects of P450 deletion(s) on cell mass of *S. venezuelae*, we measured the dry cell weights (DCWs) of *Sv*-WT, *Sv*-Del1, 21 multi-P450 knockout strains (*Sv*-Del2∼22), and the P450-null mutant *Sv*-Del23 upon 3 days of cultivation in MYM liquid media. Unexpectedly, the biomasses of all tested P450 knockout mutants were similar to each other, but significantly higher than that of *Sv*-WT (Fig. 3a). Since there was no obvious difference in the growth and morphological differentiation of P450 knockout strains on solid MYM media, we reasoned that the deletion of a large fragment and rearrangements on the genomes of these P450-deficient strains might account for the enhanced accumulation of their biomasses.

Next, we investigated whether the P450 gene knockout(s) could cause the changes in secondary metabolism. Experimentally, the 25 single P450 deletion mutants were cultured in two different liquid media (SCM and ISP4) and their metabolite profiles were comparatively analyzed by HPLC. In SCM medium, neomethymycin and methymycin were produced in high yields by *Sv*-WT, while pikromycin was not observed due to the known impact of fermentation media on product distribution [46]. Moreover, a small amount of 10-deoxymethynolide (10-dml), the aglycone of YC-17 and (neo)methymycin as well as the substrate of glycosyltransferase DesVII, was also detected (Fig. S8). As expected, the strain *Sv*-Δ*pikC* accumulated the two native substrates of PikC, namely, YC-17 and narbomycin, and the hydroxylation products (neo)methymycin and pikromycin were not detected, consistent with the previous report [28]. By contrast, the metabolic profiles of the rest 24 single P450 deletion mutants were basically the same as that of *Sv*-WT (Fig. S8). Unlike SCM medium, the wild-type strain cultured in ISP4 medium accumulate less 12-membered macrocyclic lactones (Fig. S9). In addition, compared to the wild type strain, the non-PikC P450 single deletion mutants did not synthesize different products in ISP4 media.

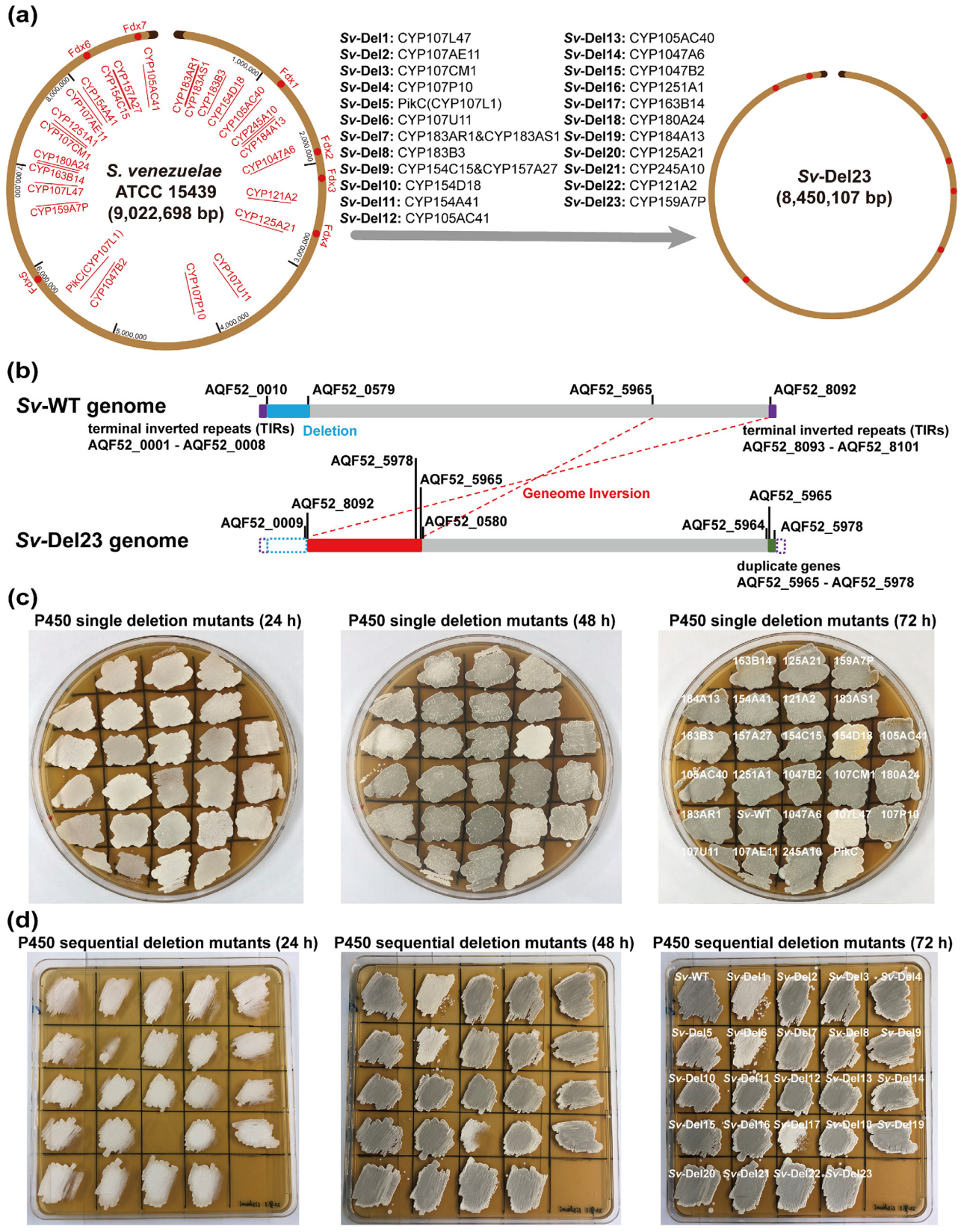

Fig. 2. Construction of single and multiple P450 deletion mutants of *S. venezuelae* ATCC 15439. (a) Genome maps of *S. venezuelae* ATCC 15439 wild type (*Sv*-WT) and the P450-free mutant (*Sv*-Del23). The locations of the targeted P450 and Fdx genes are marked with red lines and red dots, respectively. The order of sequential P450 gene deletions and the corresponding multi-P450 deletion strain names (in bold) are displayed above the arrow. (b) Chromosomal alignment of *Sv*-Del23 and *Sv*-WT. The purple dashed boxes represent the deleted TIR regions (indicated by solid purple boxes). The blue dashed box denotes the large segment deletion. The solid red box represents the translocation and inversion region. The gray solid box demonstrates the unchanged sequences. The solid green box denotes the duplicated region of AQF52_5965–AQF52_5978. (c) Phenotypes of the single P450 deletion mutants. (d) Phenotypes of the sequential P450 deletion mutants. Strains were grown on MYM agar plates and photographed after one day at a 24 h interval. The locations of the wild-type strain and different P450 deletion mutants are marked on the MYM agar plates cultured for 72 h.

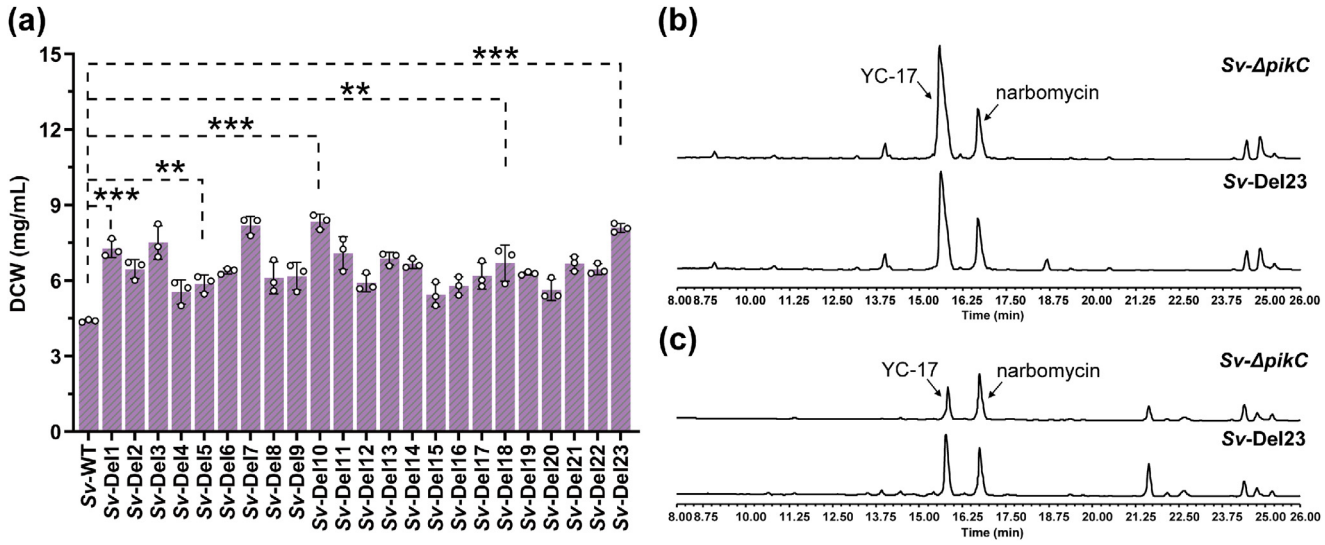

Fig. 3. Characterization of sequential P450 deletion mutant strains. (a) Dry cell weights (DCWs) of *Sv*-WT and sequential P450 deletion mutants cultured in MYM liquid media. Data are presented as mean values ± SD. Black hollow circles represent $n = 3$ individual biological samples. *P* values were determined by two-tailed unpaired *t*-test. $^{**}P < 0.01$, $^{***}P < 0.001$. (b, c) HPLC (230 nm) analysis of the fermentation extracts from *Sv*-Δ*pikC* and *Sv*-Del23 grown in SCM (b) and ISP4 (c) liquid media.

Finally, we analyzed the metabolic profiles of the P450-null mutant *Sv*-Del23 in both SCM and ISP4 media (Fig. 3b, c). Compared with *Sv*-Δ*pikC, Sv*-Del23 did not produce any notable new products under the tested culture conditions. These results indicate that, except for PikC, other P450 enzymes should have no direct relationship with secondary metabolism of *S. venezuelae* during the fermentation in SCM and ISP4 media. Supporting this, the metabolic profiles of non-PikC single P450 deletion mutants were consistent with that of *Sv*-WT (Figs. S8 and S9). Although some P450 genes are within or adjacent to BGCs, their expression was likely silent under these fermentation conditions.

3.6. The phenotypes of P450 overexpression strains

Considering the facts that 1) some P450 expression levels were low or even silent under the tested conditions; and 2) the single and multiple P450 gene knockouts did not cause significant phenotypic changes, we hypothesized that increased P450 expression might trigger some detectable changes. Thus, we individually transformed 25 P450-overexpression plasmids into *S. venezuelae* with each P450 expression driven by the constitutive *kasO*p* promoter. The 25 single P450 overexpression mutants were constructed and validated through PCR amplification (Table S1, Fig. S10). As a result, overexpression of every single P450 gene did not lead to significant morphological or metabolic changes (Figs. S11 and S12), consolidating the above conclusions drawn from the P450 knockout results (Fig. 2, Figs. S8 and S9).

3.7. Construction of Fdx-deletion and Fdx-repression mutants

Fdxs are single electron carriers that are important for many oxidoreductive processes, some of which are also responsible for sequentially delivering two catalytically required electrons from FdRs to P450s. To understand how P450s and Fdxs interact with each other inside *S. venezuelae* cells, we attempted to individually disrupt seven *fdx* genes using CRISPR/Cas9-based gene editing technology. We successfully constructed four single *fdx* deletion mutants including *Sv*-Δ*fdx1, Sv*-Δ*fdx4, Sv*-Δ*fdx6* and *Sv*-Δ*fdx7* (Table S1, Fig. S13). However, the deletion of *fdx2, fdx3* or *fdx5* turned out to be unsuccessful despite our greatest efforts, suggesting that the three *fdx* genes might be essential housekeeping genes. To confirm this, we integrated an additional copy of *fdx5* into the genome with its expression driven by the strong constitutive promoter *kasO*p*, giving rise to the recombinant strain *Sv-fdx5* × 2 (Table S1, Fig. S14). When the original copy of *fdx5* was deleted from *Sv-fdx5* × 2, the resulting strain *Sv-kasO*p*-fdx5* grew as normal, supporting that Fdx5 should be necessary for survival of *S. venezuelae*. Using the similar knockout strategy, unexpectedly, we were still unable to delete the housekeeping genes *fdx2* and *fdx3*, likely because both genes are located within a vital BGC (Figs. S15 and S16).

Our previous study revealed that the seven heterologously expressed and purified Fdxs (*i.e.*, Fdx1–7 of *S. venezuelae*) were capable of supporting the *in vitro* catalytic activity of PikC to different extents [26]. To further identify the major Fdx(s) to serve PikC *in vivo*, we sequentially inactivated the four non-essential *fdx* genes according to their *in vitro* PikC-supporting activities from low to high, giving rise to *Sv*-Δ*fdx1, Sv*-Δ*fdx16, Sv*-Δ*fdx164* and *Sv*-Δ*fdx1647* (Table S1, Fig. S17a–c). Moreover, to assess the functional importance of the housekeeping *fdx* genes towards PikC, the CRISPR/dCas9-based interference system (CRISPRi) was used to individually repress the expression of *fdx2, fdx3* and *fdx5* [30], leading to the three recombinant strains *Sv*-Δ*fdx2*-down, *Sv*-Δ*fdx3*-down and *Sv*-Δ*fdx5*-down (Table S1). The quantitative real-time PCR (qRT-PCR) clearly showed that the transcriptional levels of these three *fdx* genes were dramatically reduced (Fig. S18). Compared with *Sv*-WT, the mRNA levels of *fdx2* in the *Sv*-Δ*fdx2*-down strain were down-regulated by 97 % (24 h) and 93 % (36 h); and the corresponding percentage numbers for *fdx3* and *fdx5* were 97 % and 79 % (24 h) and 98 % and 72 % (36 h), respectively.

3.8. Evaluation of the PikC-supporting activity of Fdxs in vivo

S. venezuelae can rapidly synthesize the 12-membered ring macrolides neomethymycin, methymycin and YC-17 in SCM medium [37]. Since the relative yields of YC-17 (substrate) and (neo)methymycin (products) can be used as an indicator for PikC's activity *in vivo*, we selected PikC as a representative P450 enzyme to elucidate the cellular P450-Fdx interactions. Thus, we analyzed the metabolic profiles of the seven *fdx* mutant strains (Fig. 4). Specifically, *Sv*-WT produced abundant neomethymycin and methymycin at a ~1:1 ratio, and YC-17 was undetectable in its metabolites (Fig. 4), indicating that PikC was able to completely hydroxylate YC-17 in the wild type strain. *Sv*-Δ*fdx6* and *Sv*-Δ*fdx7* generated similar metabolic profiles as *Sv*-WT, suggesting that these two Fdxs should not be the major electron donors for PikC catalysis. Interestingly, *Sv*-Δ*fdx1* only produced very small amounts of methymycin and

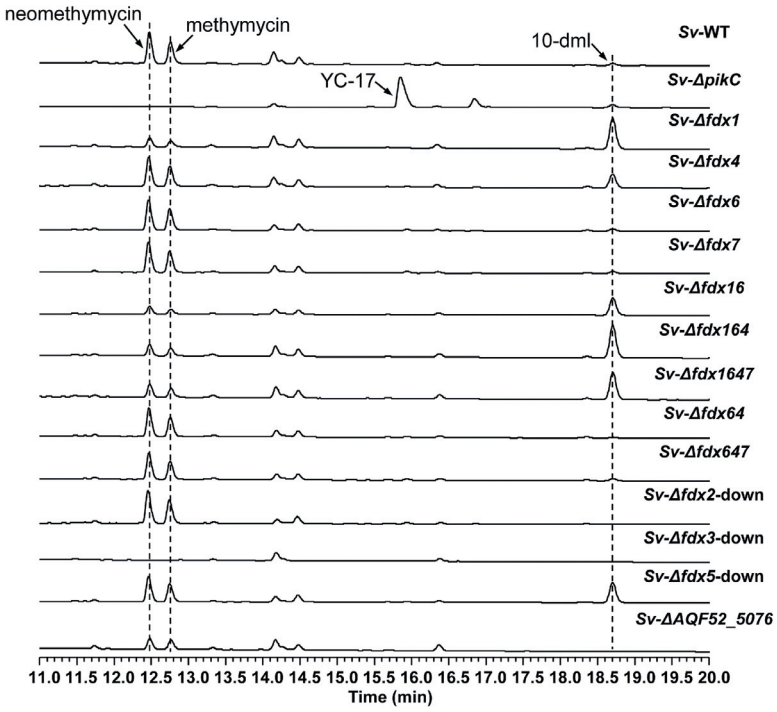

Fig. 4. Comparison of the yields of neomethymycin, methymycin, YC-17 and 10-dml. HPLC (230 nm) analysis of the fermentation extracts of *S. venezuelae* wild-type, *Sv*-Δ*pikC*, single and sequential *fdx* deletion mutants, *fdx* knockdown mutants, and *Sv*-Δ*AQF52_5076* cultured in SCM liquid media.

neomethymycin and lost the ability to accumulate YC-17; while generated 4.8 times more 10-dml than *Sv*-WT. This result suggested that the *fdx1* knockout might attenuate the glycosylation of 10-dml via some unknown mechanism. The production of 10-dml by *Sv*-Δ*fdx4* also increased 4-fold compared to *Sv*-WT (Fig. 4), but this only led to a moderate decrease in the production of neomethymycin and methymycin (Fig. 4), suggesting that Fdx4 might have a weaker regulatory effect on 10-dml glycosylation than Fdx1.

With regard to multiple *fdx* gene knockout mutants, all the three multi-*fdx* deletion mutants with *fdx1* removed (*i.e.*, the double knockout mutant *Sv*-Δ*fdx16*, the triple knockout mutant *Sv*-Δ*fdx164*, and the quadruple knockout mutant *Sv*-Δ*fdx1647*) showed the metabolic profiles similar to that of *Sv*-Δ*fdx1*, indicative of the epistatic effect of *fdx1* (Fig. 4). Differently, the metabolic profiles of the double mutants *Sv*-Δ*fdx64* and the triple mutant *Sv*-Δ*fdx647* mimicked that of *Sv*-WT (Figs. 4, S17d, e, Table S1). Taken together, these results confirmed that Fdx4, Fdx6 and Fdx7 have minor or no electron-supplying ability for PikC. Furthermore, down-regulation of *fdx2* or *fdx5* did not affect the product profile, indicating that these two housekeeping *fdx* genes are unlikely related to PikC catalysis (Fig. 4). By contrast, the *fdx3*-suppressed mutant lost the ability to synthesize any products or intermediates of the pikromycin/(neo)methymycin biosynthetic pathway (Fig. 4), suggesting that the synthesis of these antibiotics might be controlled by Fdx3 somehow. We speculated that *fdx3* might play an important positive regulatory role in expression of the polyketide synthase genes *pikA* (some or all of *pikAI-AV*) of pikromycin cluster. To test this hypothesis, we performed qRT-PCR analysis on the *pikA* genes in the *fdx3*-suppressed mutant (Figs. S19 and S20). As expected, the expression levels of *pikAI-III* and *pikAV* genes were significantly reduced or even silenced due to *fdx3* knockdown. Surprisingly, the expression level of *pikAIV* was not significantly affected, indicating that Fdx3 has differential regulatory functions for *pikAI-AV* (Fig. 5). With regard to the differences, more studies on regulatory mechanisms are required, which are currently undergoing in this laboratory. Although *pikAIV* was actively expressed, the down-regulation or silence of *pikAI-AIII* was enough to abolish the biosynthesis of the polyketide backbone.

Since Fdx1 and Fdx3 could impact the biosynthetic process prior to YC-17, we further performed the YC-17 feeding experiments to simplify our analysis. Specifically, when *Sv*-Δ*fdx1* or *Sv*-Δ*fdx3*-down was fed with 200 μM of YC-17, which was completely converted to neomethymycin and methymycin by these two mutants (Figs. S21 and S22). These results strongly suggest that the PikC-supporting activities of Fdx1 and Fdx3 could be complemented by each other (Fig. 5). Interestingly, Fdx1 and Fdx3 showed the lowest and highest PikC-supporting activities respectively in our previous *in vitro* experiments [26]. Although Fdx2, Fdx4, Fdx5, Fdx6 and Fdx7 were able to shuttle electrons for PikC *in vitro*, our results in this study (Fig. 4, Figs. S21 and S22) indicated that these Fdxs have minor or no supporting activities for PikC *in vivo*. These inconsistencies may be due to complex intracellular environments or some unknown metabolic regulation.

3.9. *Transcriptome analysis of* Sv-Δfdx1

Since *Sv*-Δ*fdx1* showed the dramatically changed metabolic profile relative to *Sv*-WT, we sought to understand the global effects of *fdx1* on *S. venezuelae* by analyzing its transcriptome at the transition phase (24 h) in SCM medium. The comparative transcriptomic analysis showed that 8,078 genes were co-expressed in *Sv*-Δ*fdx1* and *Sv*-WT (Fig. S23). The deletion of *fdx1* triggered expression of 15 genes and silenced the two genes *AQF52_0061* and *AQF52_5076* (Table S8). Additionally, compared to *Sv*-WT, 878 and 411 genes were up- and down-regulated respectively in *Sv*-Δ*fdx1* (Fig. 6a). Furthermore, the differentially expressed genes (DEGs) enrichment pathway was classified by analyzing the down- and up-regulated DEGs in Gene Ontology (GO) and Kyoto Encyclopedia of Genes and Genomes (KEGG). We revealed that down-regulated DEGs were mainly associated with the methyltransferase activity, transporter activity, the ABC transporter pathway, and primary metabolism. Up-regulated DEGs were enriched in regulation of RNA metabolic and gene expression processes, DNA binding activity, nucleotide metabolism, and biosynthesis of cofactors (Fig. S24).

However, no apparent relationship was found between the deletion of *fdx1* and the reduced macrolide antibiotic production from DEGs enrichment analysis. Of note, our analysis of *Sv*-Δ*fdx1* transcriptome data revealed that the silent gene *AQF52_5076*, encoding an *S*-adenosylmethionine synthase is located 1,478 bp downstream of the pikromycin BGC, which may potentially provide the necessary methyl group dur-

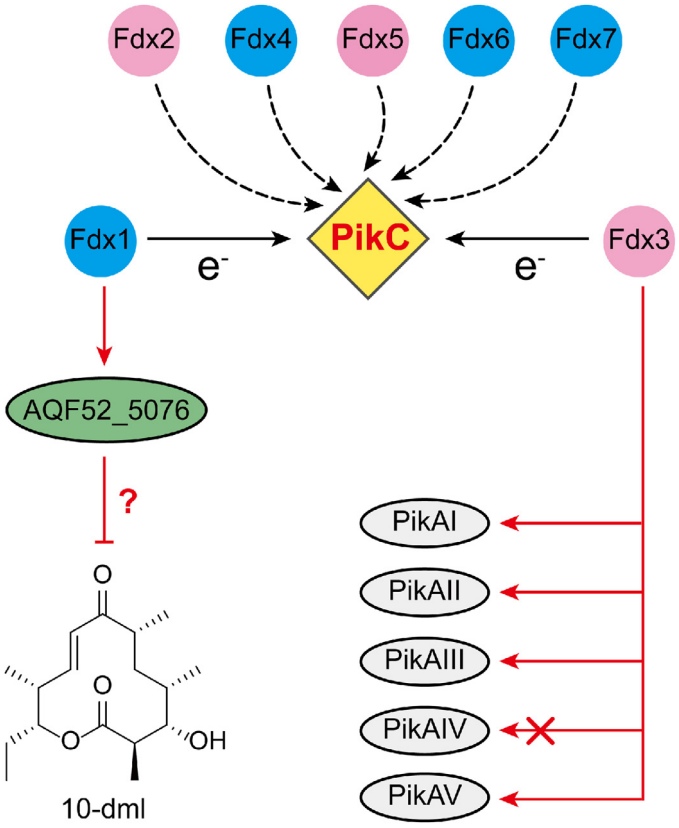

Fig. 5. The putative regulatory effects of Fdxome on biosynthesis of the 12-membered ring macrolactone/macrolides. PikAI-III, the three modular polyketide synthases responsible for assembling the linear pentaketide. PikAIV, the fourth polyketide synthase (containing a thioesterase domain) responsible for assembling the linear hexaketide and for cyclizing the linear polyketides (*see* Fig. S19 of Supplementary materials for details). PikAV, a type II thioesterase (TE II). AQF52_5076, an *S*-adenosyl-methionine synthase. Pink and blue circles represent the housekeeping and non-housekeeping *fdx* genes, respectively. Solid and dashed black arrows represent the major and minor/no electron transferring activities for PikC *in vivo*. Red solid arrows represent the positive transcriptional regulatory functions. The cross indicates no regulatory effect. The red blunt arrow denotes the inhibitory effect of AQF52_5076 on 10-dml production via unknown mechanism.

ing the biosynthesis of desosamine deoxysugar in (neo)methymycin and pikromycin that contains a dimethylamino group [37]. Thus, we constructed the *AQF52_5076* deletion mutant (Table S1, Fig. S25), and this mutant gave quite similar production of methymycin and neomethymycin to *Sv*-Δ*fdx1* (Fig. 4). However, it did not accumulate 10-dml at a detectable level. Therefore, we deduced that Fdx1 might have a transcriptional activation effect on *AQF52_5076* (Fig. 5). The decreased amounts of methymycin and neomethymycin by *Sv*-Δ*fdx1* were possibly caused by silenced *AQF52_5076*, but the detailed regulatory mechanisms for 10-dml production require further studies.

Transcriptomic analysis also showed (Fig. 6b) that the expression level of some genes related to pyruvate metabolism decreased in *Sv*-Δ*fdx1*, indicating that *fdx1* also plays some roles in primary metabolism. However, there was no significant reduction in biomass of *Sv*-Δ*fdx1* (Fig. S26), suggesting that the impaired pyruvate pathway might be complemented by other metabolic pathway(s), thus maintaining the robust growth. Notably, the deletion of *fdx1* led to up-regulation of aerial mycelia formation genes and down-regulation of the genes involved in sporulation and spore cell wall formation (Fig. 6b). Supporting this, the observation by scanning electron microscope (Fig. 6c) showed that the morphological phenotype of *Sv*-Δ*fdx1* was quite different from that of *Sv*-WT, exhibiting a trend of accelerated senescence and slowed sporulation. Meanwhile, the spore differentiation of *Sv*-Δ*fdx1* grown on MYM agar exhibited shedding and lysis of hydrophobic sheaths; and the mutant strain exhibited wrinkled cell morphology in 2 × YT liquid medium.

4. Discussion

The functions of P450s have been studied for more than 60 years [47], but little attention has been paid to functional analysis of a whole P450ome in *Streptomyces in vivo*. Although the electron transfer mediated by Fdx has been reported as the rate limiting step in P450-catalyzed reactions [48] and the *in vitro* P450-Fdx interactions have intensively been investigated in recent years [25–27,49–52], the cellular P450-Fdx interactions remains largely underexplored. To address these knowledge gaps, in this study, we systematically analyzed the physiological functions of P450ome and Fdxome in *S. venezuelae* ATCC 15439.

For the first time, we showed that all P450 genes are not essential for the survival of a streptomycete strain. The P450 genes of *S. venezuelae* ATCC 15439 are also unrelated to growth and differentiation of this bacterial strain under several tested conditions. These facts raise an intriguing question about the evolutionary implication of the non-housekeeping nature of a CYPome, especially considering that P450 superfamily is flourishing in *Streptomyces*. The non-housekeeping nature of P450 genes under relaxing conditions might have benefited the divergent evolution of P450s in *Streptomyces* during the long evolutionary history. Notably, there have been a growing number of reports on the critical functions of P450s for host microbes in toxic environments or when co-cultured with other organisms. For example, *Bacillus thuringiensis* efficiently degrades benzo(a)pyrene via P450-catalyzed hydroxylation reactions [53]. P450s in the fungus *Scedosporium* sp. participates in the degradation of tetrahydrofuran when co-cultured with other microorganisms such as *Pseudonocardia* [54]. *Rhodococcus* sp. strain NI86/21 relies on a single P450 system to degrade multiple herbicides in the living environment through dealkylation [55]. Thus, the living conditions and environmental factors of a microorganism could influence its dependence on P450 genes. Under certain circumstances, P450 genes might become conditionally essential. With no doubt, these hypotheses require further studies on evolution, ecology, and environmental toxicology of P450 enzymes. With regard to the effect of P450s on secondary metabolism, except PikC involved in the biosynthesis of macrolide antibiotics, the knockout of other P450 genes did not cause any significant disturbance of metabolic profiles. We reason that most P450 genes might be either unrelated to secondary metabolite biosynthesis, or located within a silent (*e.g.*, CYP183AR1 and CYP183AS1) or even “dead” BGC.

In the genome of the P450-free mutant *Sv*-Del23 (Fig. 2b), its linear chromosome contains large-scale DNA rearrangements including large segment deletion, inversion, translocation, and amplification, which were resulted from common genetic instability of *Streptomyces* [56]. The 0.6 Mbp deletion region contains 570 genes, including many hypothetical proteins with unknown functions and enzymes with various metabolic activities (Table S9). As reported, gene deletion often occurs along with DNA amplification [57,58]. Notably, CRISPR/Cas9 poses a deletion risk to the genes located in putatively unstable regions, thus exacerbating the instability of linear chromosomes [59]. This finding is well supported by our serial P450 gene knockout results. Moreover, chromosomal rearrangement also resulted in some off-target effects on *CYP121A2* and *CYP159A7P* gene loci during the continuous gene deletions, which had already been resolved by screening for new gRNAs (Table S1).

Based on lethality of gene deletion, we determined that *fdx2, fdx3* and *fdx5* are housekeeping ferredoxin genes of *S. venezuelae*. Similarly, previous studies have shown that a bacteria-specific 2[4Fe–4S] ferredoxin is essential in *P. aeruginosa* [24]. Ferredoxin Fd plays a central role in maintaining the function and stability of the apicoplast organelle in malaria parasites [74]. These findings provide important targets and

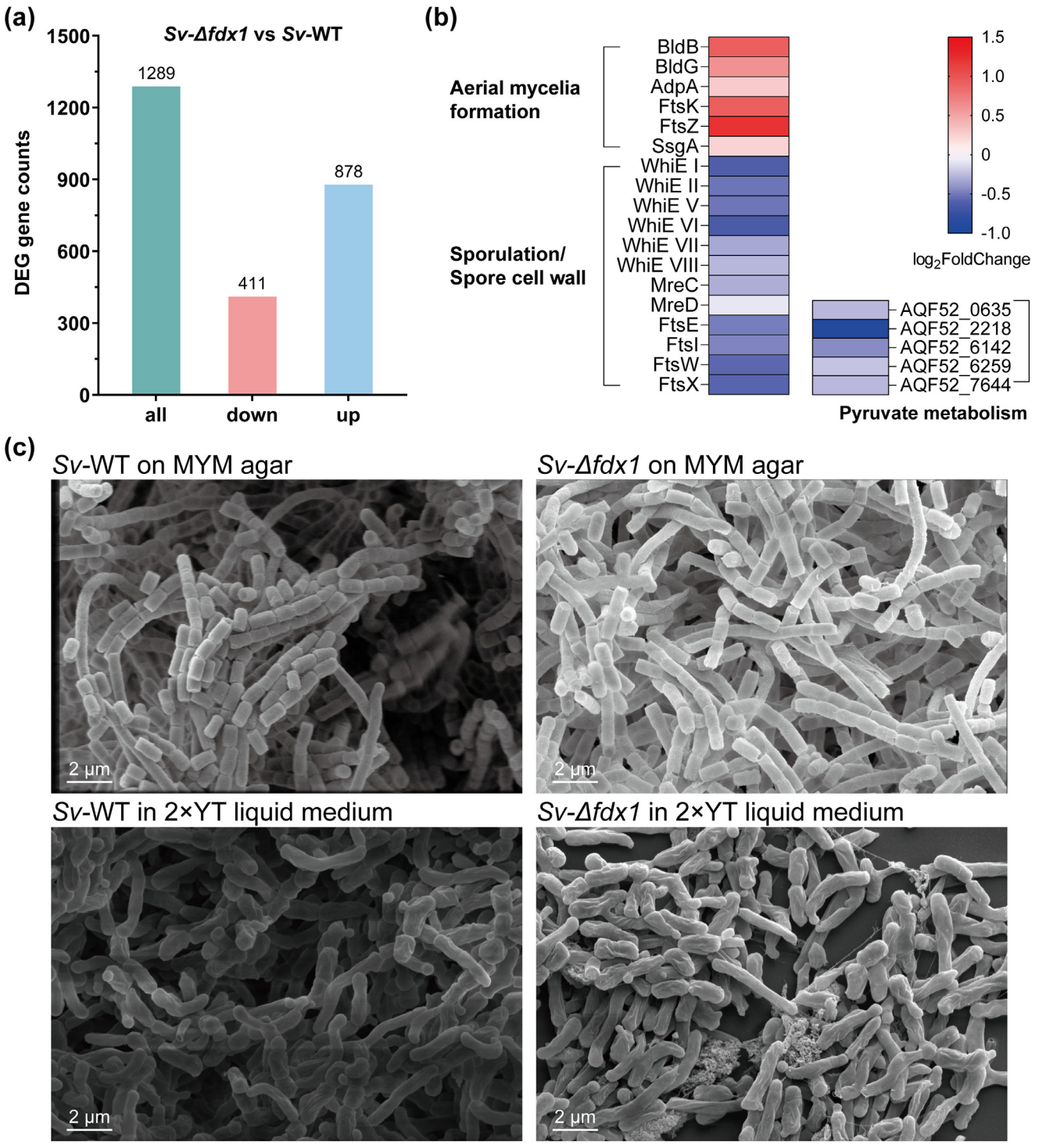

Fig. 6. Transcriptome and phenotype analyses of *Sv*-Δ*fdx1*. (a) Differentially transcribed genes in *Sv*-Δ*fdx1* and *Sv*-WT. (b) Transcriptome analysis of differentially expressed genes associated with growth, differentiation, and pyruvate metabolism in *Sv*-Δ*fdx1* compared with *Sv*-WT. Red and blue squares represent up- and down-regulated genes, respectively. (c) Field emission scanning electron micrographs (FESEM) of *Sv*-WT and *Sv*-Δ*fdx1* at × 20,000 magnification. The strains were grown on MYM agar plates and 2 × YT liquid medium at 30 °C for 3 days prior to electron microscopy observations.

directions for inhibition of pathogenic bacteria/parasites or competing strains carrying a housekeeping *fdx* gene.

In addition to the complementary PikC-supporting activities of Fdx1 and Fdx3, interestingly, we discovered the regulatory functions of these two Fdxs. The disruption of *fdx1* silenced the *S*-adenosyl-methionine synthase gene *AQF52_5076* and altered expression of morphological differentiation genes, demonstrating that Fdx1 is not only an electron transporter for P450s, but also an important transcription regulatory factor, as FNR, IscR and SoxR [60–62]. Importantly, we revealed that Fdx3 showed a direct regulatory activity on the three polyketide synthases PikAI-AIII (but not the fourth PikAIV) and the type II thioesterase PikAV. Xue *et al.* reported that in SCM medium PikAIV was expressed as an *N*-terminal truncated form [63,64]. Taken together, we hypothesized that *pikAIV* might have an alternative transcription start site, thus

enabling this gene to escape the regulation of Fdx3. Supporting this, a suspected promoter was previously reported to be located at 2 bp upstream of the coding region of *pikAIV* [65]. Of note, the unclear regulatory mechanisms of Fdx1 and Fdx3 will prompt us to use transcriptomics, proteomics, and metabonomics to elucidate the regulatory networks of these ferredoxins in *S. venezuelae* in the future. The mechanistic understandings may provide a new strategy for control of morphological development and/or for titer improvement of bioactive secondary metabolites via ferredoxin gene manipulation.

The housekeeping *fdx2* gene is located in a Pup-proteasome system (Fig. S15), which is reportedly involved in regulation of bacterial growth, differentiation, and bacterial stress response [66–68]. The deletion of *fdx2* would probably disrupt the Pupylation of iron storage protein ferritin downstream the proteasome of *S. venezuelae*, thereby resulting in host death. This is similar to how the absence of ferritin causes severe growth defects in *Corynebacterium glutamicum* [69]. As for the housekeeping *fdx3*, it is located in an iron-sulfur cluster biosynthetic system, which provides intermediates and transporter for the assembly of Fe–S cluster (Fig. S16), such as Isc, Nif, and Suf [23,70,71]. Thus, we speculate that the knockout of *fdx3* would disrupt the Fe–S cluster biosynthesis, leading to cell death [72]. The housekeeping *fdx5* gene does not belong to any gene cluster or protein complex. However, a housekeeping gene encoding an RNA polymerase σ^{70} factor, is located downstream *fdx5*, which plays an irreplaceable role in gene regulation, iron uptake, and stress survival [73]. Although it cannot be proved that the *fdx5* knockout would cause loss of function of σ^{70} factor, this is certainly an intriguing question to be addressed in the future.

In summary, we conducted a comprehensive functional analysis of the whole P450ome of *S. venezuelae* ATCC 15439 and provided significant insights into the PikC-Fdx interactions *in vivo*. A P450-free *Streptomyces* strain was constructed for the first time, which demonstrating the non-housekeeping nature of P450 enzymes. In *S. venezuelae*, P450s seem not to be relevant to cell growth and morphological differentiation. Intriguingly, Fdx1 and Fdx3 can jointly support the cellular activity of PikC. In addition to electron transfer, Fdx1 and Fdx3 have important regulatory functions in morphological development and secondary metabolism of *S. venezuelae*.

Data Availability Statement

The whole-genome sequence of *Streptomyces venezuelae* ATCC 15439 wild type (*Sv*-WT) and the P450-free strain *Sv*-Del23 were deposited into GenBank under Accession Nos. CP140569 (for *Sv*-WT) and CP140665 (for *Sv*-Del23). All other relevant data supporting the findings of this study are available in this manuscript and Supplementary Materials.

Declaration of competing interest

The authors declare the following financial interests/personal relationships which may be considered as potential competing interests: Given their roles as Executive Editor and Editorial Board Member, respectively, Dr. Shengying Li and Dr. Vlada B. Urlacher had no involvement in the peer-review of this article, and had no access to information regarding its peer-review. Full responsibility for the editorial process for this article was delegated to Dr. Linquan Bai.

CRediT authorship contribution statement

Shuai Li: Writing – review & editing, Writing – original draft, Validation, Investigation, Formal analysis, Conceptualization. **Zhong Li:** Investigation, Funding acquisition. **Guoqiang Zhang:** Formal analysis. **Vlada B. Urlacher:** Writing – review & editing. **Li Ma:** Writing – review & editing, Funding acquisition. **Shengying Li:** Writing – review & editing, Supervision, Resources, Funding acquisition, Conceptualization.

Acknowledgments

This work was supported by the National Natural Science Foundation of China (32025001, 32071266 and 32200017), the Shandong Provincial Natural Science Foundation (ZR2022QC070 and ZR2019ZD20).

Supplementary Materials

Supplementary material associated with this article can be found, in the online version, at doi:10.1016/j.engmic.2024.100166.

References

[1] D.A. Hopwood, Soil to genomics: the *Streptomyces* chromosome, Annu. Rev. Genet. 40 (2006) 1–23.
[2] K. Alam, A. Mazumder, S. Sikdar, Y. Zhao, J. Hao, C. Song, Y. Wang, R. Sarkar, S. Islam, Y. Zhang, A. Li, *Streptomyces*: the biofactory of secondary metabolites, Front. Microbiol. 13 (2022) 968053.
[3] S.B. Zotchev, Marine actinomycetes as an emerging resource for the drug development pipelines, J. Biotechnol. 158 (2012) 168–175.
[4] E.A. Barka, P. Vatsa, L. Sanchez, N. Gaveau-Vaillant, C. Jacquard, J.P. Meier-Kolthoff, H.P. Klenk, C. Clément, Y. Ouhdouch, G.P. van Wezel, Taxonomy, physiology, and natural products of *Actinobacteria*, Microbiol. Mol. Biol. Rev 80 (2016) 1–43.
[5] D.R. Nelson, T. Kamataki, D.J. Waxman, F.P. Guengerich, R.W. Estabrook, R. Feyereisen, F.J. Gonzalez, M.J. Coon, I.C. Gunsalus, O. Gotoh, K. Okuda, D.W. Nebert, The P450 superfamily: update on new sequences, gene mapping, accession numbers, early trivial names of enzymes, and nomenclature, DNA Cell Biol. 12 (1993) 1–51.
[6] J.D. Rudolf, C.Y. Chang, M. Ma, B. Shen, Cytochromes P450 for natural product biosynthesis in *Streptomyces*: sequence, structure, and function, Nat. Prod. Rep. 34 (2017) 1141–1172.
[7] T. Sakaki, Practical application of cytochrome P450, Biol. Pharm. Bull. 35 (2012) 844–849.
[8] L.M. Podust, D.H. Sherman, Diversity of P450 enzymes in the biosynthesis of natural products, Nat. Prod. Rep 29 (2012) 1251–1266.
[9] N.M. Zondo, T. Padayachee, D.R. Nelson, K. Syed, Saprophytic to pathogenic mycobacteria: loss of cytochrome P450s vis a vis their prominent involvement in natural metabolite biosynthesis, Int. J. Mol. Sci. 24 (2022) 149.
[10] J. Shin, J.E. Kim, Y.W. Lee, H. Son, Fungal cytochrome P450s and the P450 complement (CYPome) of *Fusarium graminearum*, Toxins 10 (2018) 112 (Basel).
[11] D.C. Lamb, T. Skaug, H.L. Song, C.J. Jackson, L.M. Podust, M.R. Waterman, D.B. Kell, D.E. Kelly, S.L. Kelly, The cytochrome P450 complement (CYPome) of *Streptomyces coelicolor* A3(2), J. Biol. Chem. 277 (2002) 24000–24005.
[12] D.C. Lamb, H. Ikeda, D.R. Nelson, J. Ishikawa, T. Skaug, C. Jackson, S. Omura, M.R. Waterman, S.L. Kelly, Cytochrome P450 complement (CYPome) of the avermectin-producer *Streptomyces avermitilis* and comparison to that of *Streptomyces coelicolor* A3(2), Biochem. Biophys. Res. Commun. 307 (2003) 610–619.
[13] J.Y. Song, Y.J. Yoo, S.K. Lim, S.H. Cha, J.E. Kim, J.H. Roe, J.F. Kim, Y.J. Yoon, Complete genome sequence of *Streptomyces venezuelae* ATCC 15439, a promising cell factory for production of secondary metabolites, J. Biotechnol. 219 (2016) 57–58.
[14] D.C. Lamb, M.R. Waterman, B. Zhao, *Streptomyces* cytochromes P450: applications in drug metabolism, Expert Opin. Drug Metab. Toxicol. 9 (2013) 1279–1294.
[15] M.A. Cho, S. Han, Y.R. Lim, V. Kim, H. Kim, D. Kim, *Streptomyces* cytochrome P450 enzymes and their roles in the biosynthesis of macrolide therapeutic agents, Biomol. Ther. 27 (2019) 127–133 (Seoul).
[16] S.C. Moody, E.J. Loveridge, CYP105-diverse structures, functions and roles in an intriguing family of enzymes in *Streptomyces*, J. Appl. Microbiol. 117 (2014) 1549–1563.
[17] F.C. Mnguni, T. Padayachee, W. Chen, D. Gront, J.-H. Yu, D.R. Nelson, K. Syed, More P450s are involved in secondary metabolite biosynthesis in *Streptomyces* compared to *Bacillus, Cyanobacteria*, and *Mycobacterium*, Int. J. Mol. Sci. 21 (2020) 4814–4832.
[18] L.E. Mortenson, J.E. Carnahan, R.C. Valentine, An electron transport factor from *Clostridium Pasteurianum*, Biochem. Biophys. Res. Commun. 7 (1962) 448–452.
[19] S. Li, L. Du, R. Bernhardt, Redox partners: function modulators of bacterial P450 enzymes, Trends Microbiol. 28 (2020) 445–454.
[20] Z.E. Chiliza, J. Martínez-Oyanedel, K. Syed, An overview of the factors playing a role in cytochrome P450 monooxygenase and ferredoxin interactions, Biophys. Rev. 12 (2020) 1217–1222.
[21] K.J. McLean, M. Sabri, K.R. Marshall, R.J. Lawson, D.G. Lewis, D. Clift, P.R. Balding, A.J. Dunford, A.J. Warman, J.P. McVey, A.M. Quinn, M.J. Sutcliffe, N.S. Scrutton, A.W. Munro, Biodiversity of cytochrome P450 redox systems, Biochem. Soc. Trans. 33 (2005) 796–801.
[22] H. Mustila, Y. Allahverdiyeva, J. Isojärvi, E.M. Aro, M. Eisenhut, The bacterial-type [4Fe-4S] ferredoxin 7 has a regulatory function under photooxidative stress conditions in the cyanobacterium *Synechocystis* sp. PCC 6803, Biochim. Biophys. Acta Bioenerg. 1837 (2014) 1293–1304.
[23] Y. Takahashi, M. Nakamura, Functional assignment of the ORF2-*iscS-iscU-iscA-hscB-hscA-fdx*-ORF3 gene cluster involved in the assembly of Fe-S clusters in *Escherichia coli*, J. Biochem. 126 (1999) 917–926.
[24] S. Elsen, G. Efthymiou, P. Peteinatos, G. Diallinas, P. Kyritsis, J.M. Moulis, A bacteria-specific 2[4Fe-4S] ferredoxin is essential in *Pseudomonas aeruginosa*, BMC Microbiol. 10 (2010) 271.

[25] Y.J. Chun, T. Shimada, R. Sanchez-Ponce, M.V. Martin, L. Lei, B. Zhao, S.L. Kelly, M.R. Waterman, D.C. Lamb, F.P. Guengerich, Electron transport pathway for a *Streptomyces* cytochrome P450: cytochrome P450 105D5-catalyzed fatty acid hydroxylation in *Streptomyces coelicolor* A3(2), J. Biol. Chem. 282 (2007) 17486–17500.
[26] W. Zhang, L. Du, F. Li, X. Zhang, Z. Qu, L. Hang, Z. Li, J. Sun, F. Qi, Q. Yao, Y. Sun, C. Geng, S. Li, Mechanistic insights into interactions between bacterial class I P450 enzymes and redox partners, ACS Catal. 8 (2018) 9992–10003.
[27] X. Liu, F. Li, T. Sun, J. Guo, X. Zhang, X. Zheng, L. Du, W. Zhang, L. Ma, S. Li, Three pairs of surrogate redox partners comparison for class I cytochrome P450 enzyme activity reconstitution, Commun. Biol. 5 (2022) 791.
[28] Y. Xue, D. Wilson, L. Zhao, H. Liu, D.H. Sherman, Hydroxylation of macrolactones YC-17 and narbomycin is mediated by the *pikC*-encoded cytochrome P450 in *Streptomyces venezuelae*, Chem. Biol. 5 (1998) 661–667.
[29] H. Huang, G. Zheng, W. Jiang, H. Hu, Y. Lu, One-step high-efficiency CRISPR/Cas9-mediated genome editing in *Streptomyces*, Acta Biochim. Biophys. Sin. 47 (2015) 231–243.
[30] Y. Zhao, L. Li, G. Zheng, W. Jiang, Z. Deng, Z. Wang, Y. Lu, CRISPR/dCas9-mediated multiplex gene repression in *Streptomyces*, Biotechnol. J. 13 (2018) e1800121.
[31] K. Blin, S. Shaw, A.M. Kloosterman, Z. Charlop-Powers, G.P. van Wezel, M.H. Medema, T. Weber, antiSMASH 6.0: improving cluster detection and comparison capabilities, Nucleic Acids Res. 49 (2021) W29–W35.
[32] P. Gouet, E. Courcelle, D.I. Stuart, F. Métoz, ESPript: analysis of multiple sequence alignments in PostScript, Bioinformatics 15 (1999) 305–308.
[33] T. Kieser, M.J. Bibb, K.F. Chater, M.J. Butter, D.A. Hopwood, M. Bittner, Practical *Streptomyces* genetics: a laboratory manual, John Innes Foundation Norwich 291 (2000).
[34] Z. Li, Y. Jiang, X. Zhang, Y. Chang, S. Li, X. Zhang, S. Zheng, C. Geng, P. Men, L. Ma, Y. Yang, Z. Gao, Y. Tang, S. Li, Fragrant venezuelaenes A and B with a 5–5–6–7 tetracyclic skeleton: discovery, biosynthesis, and mechanisms of central catalysts, ACS Catal. 10 (2020) 5846–5851.
[35] K.J. Livak, T.D. Schmittgen, Analysis of relative gene expression data using real-time quantitative PCR and the 2(-Delta Delta C(T)) method, Methods 25 (2001) 402–408.
[36] J.E. Kim, J.S. Choi, J.H. Roe, Growth and differentiation properties of pikromycin-producing *Streptomyces venezuelae* ATCC 15439, J. Microbiol. 57 (2019) 388–395.
[37] Y. Xue, L. Zhao, H. Liu, D.H. Sherman, A gene cluster for macrolide antibiotic biosynthesis in *Streptomyces venezuelae*: architecture of metabolic diversity, Proc. Natl. Acad. Sci. U. S. A. 95 (1998) 12111–12116.
[38] Y. Xue, D.H. Sherman, Biosynthesis and combinatorial biosynthesis of pikromycin-related macrolides in *Streptomyces venezuelae*, Metab. Eng. 3 (2001) 15–26.
[39] Z. Li, L. Zhang, K. Xu, Y. Jiang, J. Du, X. Zhang, L. Meng, Q. Wu, L. Du, X. Li, Y. Hu, Z. Xie, X. Jiang, Y. Tang, R. Wu, R. Guo, S. Li, Molecular insights into the catalytic promiscuity of a bacterial diterpene synthase, Nat. Commun. 14 (2023) 4001.
[40] S. Li, L. Chi, Z. Li, M. Liu, R. Liu, M. Sang, X. Zheng, L. Du, W. Zhang, S. Li, Discovery of venediols by activation of a silent type I polyketide biosynthetic gene cluster in *Streptomyces venezuelae* ATCC 15439, Tetrahedron 126 (2022) 133072.
[41] R.J. Gurbiel, C.J. Batie, M. Sivaraja, A.E. True, J.A. Fee, B.M. Hoffman, D.P. Ballou, Electron-nuclear double resonance spectroscopy of 15N-enriched phthalate dioxygenase from Pseudomonas cepacia proves that two histidines are coordinated to the [2Fe-2S] Rieske-type clusters, Biochemistry 28 (1989) 4861–4871.
[42] Z. Chen, Y. Yu, Z. Zuo, J.B. Nelson, G.k. Michalopoulos, S. Monga, S. Liu, G. Tseng, J. Luo, Targeting genomic rearrangements in tumor cells through Cas9-mediated insertion of a suicide gene, Nat. Biotechnol. 35 (2017) 543–550.
[43] G.P. van Wezel, K.J. McDowall, The regulation of the secondary metabolism of *Streptomyces*: new links and experimental advances, Nat. Prod. Rep. 28 (2011) 1311–1333.
[44] G. Liu, K.F. Chater, G. Chandra, G. Niu, H. Tan, Molecular regulation of antibiotic biosynthesis in *streptomyces*, Microbiol, Mol. Biol. Rev. 77 (2013) 112–143.
[45] Z. Tian, Q. Cheng, F.K. Yoshimoto, L. Lei, D.C. Lamb, F.P. Guengerich, Cytochrome P450 107U1 is required for sporulation and antibiotic production in *Streptomyces coelicolor*, Arch. Biochem. Biophys. 530 (2013) 101–107.
[46] R.H. Lambalot, D.E. Cane, Isolation and characterization of 10-deoxymethynolide produced by *Streptomyces venezuelae*, J. Antibiot. 45 (1992) 1981–1982.
[47] M. Klingenberg, Pigments of rat liver microsomes, Arch. Biochem. Biophys. 75 (1958) 376–386.
[48] F.P. Guengerich, Rate-limiting steps in cytochrome P450 catalysis, Biol. Chem. 383 (2002) 1553–1564.
[49] T. Sagadin, J.L. Riehm, M. Milhim, M.C. Hutter, R. Bernhardt, Binding modes of CYP106A2 redox partners determine differences in progesterone hydroxylation product patterns, Commun. Biol. 1 (2018) 99.
[50] F. Kern, T.K.F. Dier, Y. Khatri, K.M. Ewen, J.P. Jacquot, D.A. Volmer, R. Bernhardt, Highly efficient CYP167A1 (EpoK) dependent epothilone B formation and production of 7-ketone epothilone D as a new epothilone derivative, Sci. Rep. 5 (2015) 14881.
[51] L. Ma, L. Du, H. Chen, Y. Sun, S. Huang, X. Zheng, E.S. Kim, S. Li, Reconstitution of the *in vitro* activity of the cyclosporine-specific P450 hydroxylase from *Sebekia benihana* and development of a heterologous whole-cell biotransformation system, Appl. Environ. Microbiol. 81 (2015) 6268–6275.
[52] W. Zhang, Y. Liu, J. Yan, S. Cao, F. Bai, Y. Yang, S. Huang, L. Yao, Y. Anzai, F. Kato, L.M. Podust, D.H. Sherman, S. Li, New reactions and products resulting from alternative interactions between the P450 enzyme and redox partners, J. Am. Chem. Soc. 136 (2014) 3640–3646.
[53] Q. Lu, K. Chen, Y. Long, X. Liang, B. He, L. Yu, J. Ye, Benzo(a)pyrene degradation by cytochrome P450 hydroxylase and the functional metabolism network of *Bacillus thuringiensis*, J. Hazard. Mater. 366 (2019) 329–337.
[54] M. Qi, H. Huang, Y. Zhang, H. Wang, H. Li, Z. Lu, Novel tetrahydrofuran (THF) degradation-associated genes and cooperation patterns of a THF-degrading microbial community as revealed by metagenomic, Chemosphere 231 (2019) 173–183.
[55] I. Nagy, F. Compernolle, K. Ghys, J. Vanderleyden, R. Demot, A single cytochrome-P-450 system is involved in degradation of the herbicides Eptc (S-Ethyl Dipropylthiocarbamate) and atrazine by *Rhodococcus* Sp strain Ni86/21, Appl. Environ. Microbiol. 61 (1995) 2056–2060.
[56] J.N. Volff, J. Altenbuchner, Genetic instability of the *Streptomyces* chromosome, Mol. Microbiol. 27 (1998) 239–246.
[57] P. Dyson, H. Schrempf, Genetic Instability and DNA Amplification in *Streptomyces lividans* 66, J. Bacteriol. 169 (1987) 4796–4803.
[58] U. Hornemann, C.J. Otto, X.Y. Zhang, DNA amplification in *Streptomyces achromogenes* subsp. rubradiris is accompanied by a deletion, and the amplified sequences are conditionally stable and can be eliminated by two pathways, J. Bacteriol. 171 (1989) 5817–5822.
[59] P. Leblond, B. Decaris, New insights into the genetic instability of *Streptomyces*, FEMS Microbiol. Lett. 123 (1994) 225–232.
[60] E.T. Ralph, C. Scott, P.A. Jordan, A.J. Thomson, J.R. Guest, J. Green, Anaerobic acquisition of [4Fe 4S] clusters by the inactive FNR(C20S) variant and restoration of activity by second-site amino acid substitutions, Mol. Microbiol. 39 (2001) 1199–1211.
[61] C.J. Schwartz, J.L. Giel, T. Patschkowski, C. Luther, F.J. Ruzicka, H. Beinert, P.J. Kiley, IscR, an Fe-S cluster-containing transcription factor, represses expression of *Escherichia coli* genes encoding Fe-S cluster assembly proteins, Proc. Natl. Acad. Sci. U. S. A. 98 (2001) 14895–14900.
[62] B. Demple, H. Ding, M. Jorgensen, *Escherichia coli* SoxR protein: sensor/transducer of oxidative stress and nitric oxide, Methods Enzymol. 348 (2002) 355–364.
[63] Y. Xue, D. Wilson, D.H. Sherman, Genetic architecture of the polyketide synthases for methymycin and pikromycin series macrolides, Gene 245 (2000) 203–211.
[64] Y. Xue, D.H. Sherman, Alternative modular polyketide synthase expression controls macrolactone structure, Nature 403 (2000) 571–575.
[65] D.J. Wilson, Y. Xue, K.A. Reynolds, D.H. Sherman, Characterization and analysis of the PikD regulatory factor in the pikromycin biosynthetic pathway of *Streptomyces venezuelae*, J. Bacteriol. 183 (2001) 3468–3475.
[66] N.H. Bhat, R.H. Vass, P.R. Stoddard, D.K. Shin, P. Chien, Identification of ClpP substrates in *Caulobacter crescentus* reveals a role for regulated proteolysis in bacterial development, Mol. Microbiol. 88 (2013) 1083–1092.
[67] W.K. Smits, C.C. Eschevins, K.A. Susanna, S. Bron, O.P. Kuipers, L.W. Hamoen, Stripping Bacillus: comK auto-stimulation is responsible for the bistable response in competence development, Mol. Microbiol. 56 (2005) 604–614.
[68] A. Battesti, N. Majdalani, S. Gottesman, The RpoS-mediated general stress response in *Escherichia coli*, Annu. Rev. Microbiol. 65 (2011) 189–213.
[69] A. Küberl, T. Polen, M. Bott, The pupylation machinery is involved in iron homeostasis by targeting the iron storage protein ferritin, Proc. Natl. Acad. Sci. U. S. A. 113 (2016) 4806–4811.
[70] M.R. Jacobson, K.E. Brigle, L.T. Bennett, R.A. Setterquist, M.S. Wilson, V.L. Cash, J. Beynon, W.E. Newton, D.R. Dean, Physical and genetic map of the major *nif* gene cluster from *Azotobacter vinelandii*, J. Bacteriol. 171 (1989) 1017–1027.
[71] J. Pérard, S. Ollagnier de Choudens, Iron-sulfur clusters biogenesis by the SUF machinery: close to the molecular mechanism understanding, J. Biol. Inorg. Chem. 23 (2018) 581–596.
[72] D.R. Crooks, N. Maio, A.N. Lane, M. Jarnik, R.M. Higashi, R.G. Haller, Y. Yang, T.W. Fan, W.M. Linehan, T.A. Rouault, Acute loss of iron-sulfur clusters results in metabolic reprogramming and generation of lipid droplets in mammalian cells, J. Biol. Chem. 293 (2018) 8297–8311.
[73] D. Missiakas, S. Raina, The extracytoplasmic function sigma factors: role and regulation, Mol. Microbiol. 28 (1998) 1059–1066.
[74] R.P. Swift, K. Rajaram, R. Elahi, H.B. Liu, S.T. Prigge, Roles of ferredoxin-dependent proteins in the apicoplast of *Plasmodium falciparum* parasites, mBio 13 (2021) e0302321.